ELSEVIER

Catalysis Today 63 (2000) 283–289

CATALYSIS TODAY

www.elsevier.com/locate/cattod

The influence of surface defects on ethanol dehydrogenation versus dehydration on the $UO_2(1\,1\,1)$ surface

S.V. Chong [a], M.A. Barteau [b], H. Idriss [a,*]

[a] Department of Chemistry, Materials Chemistry, University of Auckland, Private Bag 92019, Auckland, New Zealand
[b] Department of Chemical Engineering, University of Delaware, Newark, DE 19716, USA

Abstract

The decomposition of ethanol has been investigated on Ar^+-sputtered surfaces of a $UO_2(1\,1\,1)$ single crystal. X-ray photoelectron spectroscopy (XPS) of the U 4f peaks after sputtering for 1 h showed the presence of two distinct oxidation states: U^{4+} (U $4f_{7/2}$ at 380.2 eV) and U^0 (U $4f_{7/2}$ at 377.4 eV). Upon ethanol exposure at room temperature, the peak at 377.4 eV was attenuated, indicating that U^0 sites were oxidized to U^{x+i} $(x \leq 4)$. The presence of a mixture of oxidation states on the surface influenced the reaction products observed during temperature programmed desorption (TPD). While ethylene and acetaldehyde desorbed in one temperature domain (at 560 K) from stoichiometric $UO_2(1\,1\,1)$, an additional desorption domain (at 475 K) was observed over the substoichiometric surface. The ratio of acetaldehyde to ethylene produced was different in the two temperature domains. While this ratio was near unity for the 560 K domain, it decreased to ca. 0.5 for the 475 K peaks on the substoichiometric surface. The lower temperature reaction channel is likely associated with surface oxygen vacancies, as it leads to greater oxygen abstraction, forming ethylene from surface ethoxide species.

Keywords: Ethanol dehydrogenation; Ar^+-sputtered surfaces; $UO_2(1\,1\,1)$; Ethanol dehydration; Surface oxidation

1. Introduction

The use of well-defined single crystal surfaces to study reactions of relevance to heterogeneous catalysis has been carried out for more than three decades. By examination of such systems with powerful surface spectroscopic techniques, such as LEED, AES, XPS, HREELS and STM, to name a few, the properties of the substrate and/or adsorbed species which govern a particular reaction can often be elucidated. While the usual procedure, as a first step, is to carry out reactions on stoichiometric, clean and ideally defect-free surfaces, modified surfaces may also provide important insights into surface structure-reactivity relationships. Methods of surface modification may include predosing the surface with various atoms or molecules (e.g., reaction of ethanol on $H/Cu_2O(0\,0\,1)$ [1], $H_2O/TiO_2(1\,1\,0)$ [2], and $Pd/SnO_2(1\,1\,0)$ [3] surfaces). Surface composition and structural changes may be created, e.g., electron beam sputtering [4], Ar^+-bombardment [2], and most recently electron beam lithography [5] have also been employed in studies of surface reactivity.

Previously, the reactions of ethanol on stoichiometric and oxygen-predosed $UO_2(1\,1\,1)$ single crystal surfaces have been reported [6]. Two reaction pathways were observed on the stoichiometric surface — dehydration to ethylene and dehydrogenation to acetaldehyde — with a ratio of these two products of near unity. Predosing the surface with oxygen was found to

---

* Corresponding author. Tel.: +64-9-3737599;
fax: +64-9-3737422.
E-mail address: h.idriss@auckland.ac.nz (H. Idriss).

0920-5861/00/$ – see front matter
PII: S0920-5861(00)00470-3

alter neither the selectivity nor the yield of the dehydrogenation/dehydration reactions. The absence of an effect of predosing the surface with oxygen (>100 L) at room temperature was attributed to the fact that the surface of $UO_2(1\,1\,1)$ is oxygen terminated [7,8]. Furthermore, STM studies by other workers [9] have indicated that additional adsorbed oxygen atoms are positioned at the interstitial sites of the surface. Taking into account these two factors, we have postulated that adsorbed oxygen is easily displaced from the surface by ethanol, and thus is not present to influence the reaction pathways for ethanol in TPD experiments [6].

In this paper, we report a study of the reaction of ethanol on the Ar^+-bombarded surface of $UO_2(1\,1\,1)$ single crystal, employing X-ray photoelectron spectroscopy (XPS) and temperature programmed desorption (TPD). TPD results show that, in addition to products obtained via dehydrogenation and dehydration pathways, products formed via reductive coupling and ketonisation are also observed. The operation of these reaction pathways is supported by the presence of surface acetate, acetaldehyde and ethoxide species, identified via XPS measurements on this reduced surface.

2. Experimental

The experiments were carried out in a VG Scientific surface analysis system at the University of Delaware. This system is equipped with a twin-anode X-ray source, a hemispherical energy analyser, a quadrupole mass spectrometer, LEED optics, and an argon ion sputter gun; the typical base pressure is $\sim 2\times 10^{-10}$ mbar. The $UO_2(1\,1\,1)$ single crystal was mounted onto the sample manipulator via tantalum clips holding the edges of the crystal. Two tantalum wires were spot welded onto the back of the tantalum holder to provide resistance heating, and the temperature of the sample was monitored with a chromel–alumel thermocouple glued onto the side of the crystal with high temperature cement. Mg Kα radiation ($h\nu = 1248.2$ eV) was used as the excitation source during all XPS experiments. The X-ray source was operated with a 20 mA emission current and a 15 keV acceleration voltage. All XP spectra were referenced to the O^{2-} 1s binding energy of 530.1 eV. The sample was prepared as described previously [6]. After system bake-out (408 K for 8 h), surface contaminants were removed by repeated vacuum annealing and argon ion bombardment until XPS did not show any significant amount of carbon-containing species. Reagent grade ethanol used for temperature dependent XPS and TPD experiments was subject to several freeze-pump-thaw cycles to remove volatile contaminants. All dosing was carried out at room temperature through a dosing needle connected to a variable leak valve. A heating rate of 0.90 ± 0.05 K/s was employed in all temperature programmed experiments. Quantitative TPD analyses were performed as previously described in [6]. All XPS measurements were conducted at room temperature with the sample at $\theta = 90^\circ$ from the analyser.

3. Results

3.1. Surface characterisation

The $UO_2(1\,1\,1)$ single crystal used in these experiments has been previously characterised via LEED and AES [6]. LEED has shown a (1×1) surface termination, while AES indicated the presence of five major uranium peaks at 73, 84, 94, 106 and 294 eV, as well as an O peak at 514 eV. Similar LEED patterns were also obtained after several cycles of Ar^+-bombardment and annealing in 1×10^{-7} mbar of oxygen prior to the following experiments.

3.2. TPD

Ethanol TPD following an 11 L exposure of the sputtered $UO_2(1\,1\,1)$ surface (Fig. 1) shows reactant/products desorbing in four temperature regions. Unreacted ethanol (*m*/*z* 31, 45) desorbed in a small peak that appears as a shoulder at ca. 375–390 K. The second desorption regime at ca. 475 K involved acetaldehyde (*m*/*z* 29, 43, 44), ethylene (*m*/*z* 28, 27, 26), and a C_4 product that we identify as butene (*m*/*z* 56, 55; ca. 460 K), in addition to ethanol. At ca. 530–560 K, two additional products were observed: ketene (*m*/*z* 42, 14; ca. 530 K) and acetone (*m*/*z* 58, 15; ca. 535 K), together with ethanol, ethylene, and acetaldehyde. The signal for carbon dioxide increased throughout the temperature ramp with a noticeable peak at ca. 715 K.

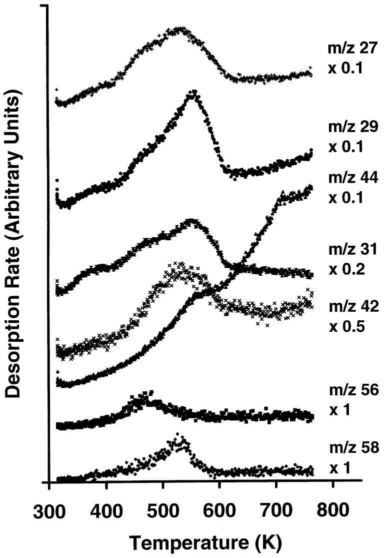

Fig. 1. Products/reactant desorption profile for ethanol TPD from a $UO_2(1\,1\,1)$ single crystal that had been Ar^+-sputtered for 1 h. The surface was exposed to ca. 11 L of ethanol vapour.

Product yield analysis indicated that 83% of the ethanol molecules initially adsorbed were converted to other products (Table 1). The main products were ethylene and acetaldehyde, accounting for 92% of the total product distribution. The ratios of acetaldehyde to ethylene were 0.53 for the reaction channel at 475 K and 0.96 for that at 560 K. Acetone and butene accounted for 3.9 and 2.7%, respectively of the carbon content of the initially adsorbed ethanol layer. Carbon dioxide could not be accurately measured but represents a product yield of the order of few per cent.

3.3. XPS

3.3.1. Sputtered and non-sputtered surfaces of the $UO_2(1\ 1\ 1)$ single crystal

XPS of the U 4f region before and after 1-h Ar^+-sputtering are shown in Fig. 2. On the non-sputtered surface the binding energies of U $4f_{7/2}$ and U $4f_{5/2}$ are positioned at 380.2 and 390.0 eV, respectively, and both peaks are accompanied by satellites at higher binding energies (ca. 7.1 eV). The full-width-half-maximum (FWHM) for both peaks was 2.0 eV. The U 4f peak positions are comparable to those obtained by Allen et al. [10] on a clean $UO_2(1\,1\,1)$ surface with the exception of the FWHM which was 0.2 eV lower compared to their results. They were also very similar to those reported for powder UO_2 (formed by H_2-reduction of α-U_3O_8) [11].

After the surface was sputtered for an hour, the base of both peaks was observed to have broadened considerably towards the lower binding energy side. This and the increase in FWHM (2.5 eV) indicated the presence of lower oxidation state uranium. Deconvolution of the U $4f_{7/2}$ peak shows the presence of a peak at ca. 377.4 eV, which can be assigned as either U^{2+} (in the form of UO) or metallic uranium. We assign the peak to U^0 as it is close to the pure uranium $4f_{7/2}$ values of 377.0 [12] and 377.3 eV [13]. No reference data for the U 4f lines of U^{2+} are available, and we do not observe any evidence for the O 1s line at 535.7 eV

Table 1
Product distribution from ethanol-TPD after ca. 11 L ethanol exposure at room temperature on the Ar^+-sputtered (1 h) surface of a $UO_2(1\,1\,1)$ single crystal

Products/reactant	Peak temperature (K)	Carbon yield (%)	Carbon selectivity (%)
Ethanol (*m*/*z* 31)	375	3.2	–
Ethanol (*m*/*z* 31)	475	5.4	–
Acetaldehyde (*m*/*z* 29)	475	7.5	9
Ethylene (*m*/*z* 27)	475	14	16.9
Butene (*m*/*z* 56)	460	2.2	2.7
Ketene (*m*/*z* 42)	530	1	1.2
Acetone (*m*/*z* 58)	535	3.2	3.9
Ethylene (*m*/*z* 27)	540	28	33.8
Ethanol (*m*/*z* 31)	560	8.6	–
Acetaldehyde (*m*/*z* 29)	560	26.9	32.5
Carbon dioxide (*m*/*z* 44)	715	n.c.[a]	n.c.

[a] Not calculated.

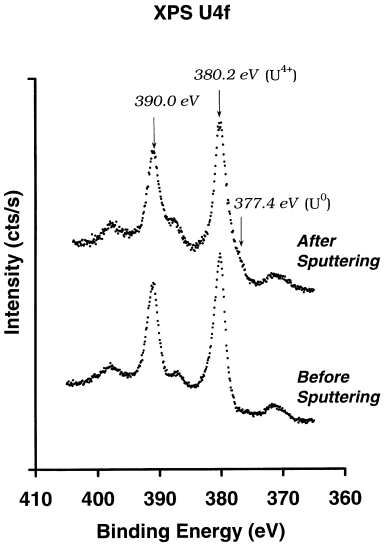

Fig. 2. XPS of U 4f peaks after 1 h of Ar^+-bombardment. The peaks at 380.2 and 390.0 eV are those of U $4f_{7/2}$ and U $4f_{5/2}$, respectively, while the shoulder at the lower binding energy side of U $4f_{7/2}$ (377.4 eV) has been assigned to the zero oxidation state of uranium.

that has been reported for UO [12]. Upon dosing of ethanol, Fig. 3, XPS U 4f analysis showed a decrease of the peak assigned to U^0. This may indicate that part of ethanol adsorption was achieved via oxygen donation to fill surface oxygen vacancies, resulting in oxidation of U^0 to $U^{x+} (x \leq 4)$.

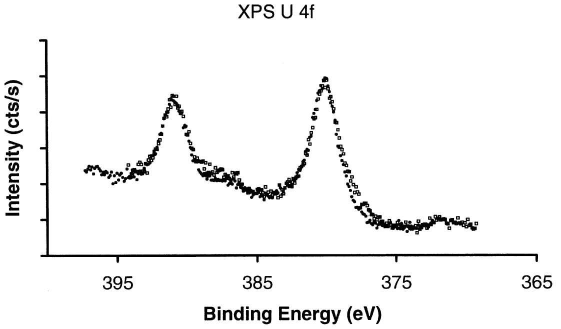

Fig. 3. Comparison between the XPS U 4f peaks before (☐) and after (●) ethanol dosing (2 L) at room temperature on the Ar^+-sputtered surface of a $UO_2(1\,1\,1)$ single crystal. Note the base of both U $4f_{7/2}$ and U $4f_{5/2}$ peaks became narrower after ethanol exposure.

XPS of the O 1s region showed no significant changes before and after sputtering. However, the C 1s spectra showed the existence of traces of carbon-containing species around 282.3–282.7 eV on both the sputtered and non-sputtered surfaces, which might be attributed to UC. The formation of uranium carbide has been reported on the surface of U metal after vacuum annealing [12,14], as well as after the reaction of methanol [15].

3.3.2. Temperature dependent XPS

3.3.2.1. C 1s. After dosing 10 L of ethanol on the sputtered surface at room temperature, the C 1s spectrum shows peaks at 285.6 eV and a shoulder at 286.5 eV, which can be assigned to the CH_3– and –CH_2O groups, respectively, of surface ethoxide species. These peaks are not assigned to molecularly adsorbed ethanol, as this species should give a peak separation close to 1.4 eV (gaseous ethanol). For example, molecularly absorbed ethanol on a $TiO_2(0\,0\,1)$ single crystal surface [16] gave rise to peaks at 286.1 and 287.5 eV (a separation of 1.4 eV), and that on $ZnO(0\,0\,0\,1)$ single crystal [17] gave a separation of 1.5 eV.

Upon heating the sample to 424 K, the peak positions remained unchanged, although C 1s peak area calculations showed that around 28% of the initial adsorbates had been removed from the surface. After heating to 497 K, the peak at 286.5 eV shifted by 0.7 to higher binding energy, and a slight rise in the signal developed at 290.2 eV. The shift to higher binding energy of the peak at 286.5–287.2 eV may be indicative of the presence of an aldehyde species. The peak at 290.2 eV may be due to surface carboxylates, as the temperature at which it is most prominent coincides with leading edge of ketene desorption in TPD experiments. Acetate species were previously observed on the surfaces of faceted $TiO_2(0\,0\,1)$ [18] and $MgO(1\,0\,0)$ [19] single crystals; in both cases the C 1s peak for the carboxylate group was located at 290.0 eV. However, the peak at 285.6 eV remained unchanged below 600 K in Fig. 4. The intensity of the peak at 287.2 attenuated slightly after heating the sample to 598 K. At this temperature, TPD shows the desorption of the remaining ketene, acetaldehyde and acetone. After heating to 722 K, an appreciable level of carbon-containing species remained

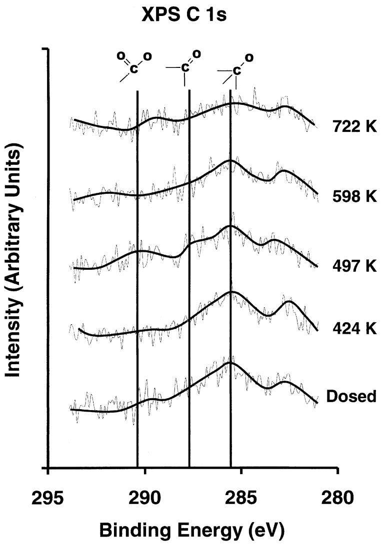

Fig. 4. C 1s spectra for a $UO_2(1\,1\,1)$ single crystal surface, Ar^+-bombarded for 1 h, exposed to 10 L of ethanol at room temperature, and heated sequentially to the temperatures indicated.

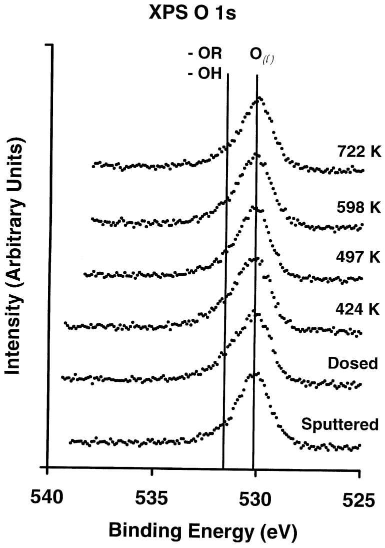

Fig. 5. Temperature dependent O 1s XPS after 10 L ethanol exposure on Ar^+-sputtered $UO_2(1\,1\,1)$ single crystal surface.

on the surface, ca. 23% of the ethanol originally adsorbed, part of which was oxidised to CO_2 as shown in Fig. 1.

3.3.2.2. O 1s. O 1s spectra were also collected to probe the surface species present with increasing temperature after ethanol exposure (Fig. 5). Prior to dosing (after sputtering for 1 h), the O 1s spectrum shows a lattice oxygen peak at 530.1 eV with a FWHM of ca. 1.8 eV. After ethanol exposure at room temperature, an asymmetric peak was produced with a shoulder at higher binding energy and a FWHM of ca. 2.2 eV. The increase in the FWHM value indicates the presence of an oxygen-containing adsorbate, most probably the ethoxide, as the binding energy difference between the lattice oxygen peak and the shoulder at higher binding energy was 1.2–1.4 eV.

The ratio of the intensity of the shoulder at higher binding energy to that of lattice oxygen might be of help in probing the reaction, and complement the C 1s and TPD studies. After heating the sample to 424 K, the ratio of the intensity of the shoulder to that of lattice oxygen at 530.1 eV decreased from 0.57:1 (at room temperature) to 0.49:1. Subsequent heating caused the intensity of the shoulder and the FWHM to decrease and at 722 K the FWHM was restored to 1.8 eV. No clear transition from surface ethoxide to surface acetate species could be resolved in the O 1s spectra, although it has previously been observed that alkoxide and carboxylate species exhibit very similar O 1s binding energies on other oxide surfaces [20].

4. Discussion

The reactions of ethanol on a stoichiometric $UO_2(1\,1\,1)$ single crystal surface were previously investigated [6]. Ethanol was converted to ethylene by dehydration and to acetaldehyde by dehydrogenation. Both products desorbed at 575 K with an acetaldehyde to ethylene ratio of ∼0.8. In the present work it was found that ethanol reacts over substoichiometric $UO_2(1\,1\,1)$ also to give mainly acetaldehyde and ethylene. However, both products desorbed in two different temperature domains: at 475 and 540–560 K. As shown in Fig. 3, the U 4f peaks in XPS become narrower upon dosing of ethanol, clearly indicating the contribution of surface defects (and their depletion by the reaction). Thus, from the results of this work and those of Ref. [6], one may conclude the following:

- non-defected $UO_2(1\,1\,1)$ single crystal surfaces exhibit a single channel for ethoxide decomposition which produces nearly equimolar amounts of dehydration and dehydrogenation products: $CH_3CHO/CH_2CH_2 = 0.96$, $T_p \approx 575\,K$;
- on oxygen deficient $UO_{2-x}(1\,1\,1)$ surfaces, a second pathway for ethoxide decomposition is opened that produces greater amounts of dehydration than dehydrogenation products: $CH_3CHO/CH_2CH_2 = 0.53$, $T_p \sim 460–480\,K$.

The shift in the reaction selectivity is most likely due to the creation of oxygen vacancies (during Ar^+-sputtering) that are restored by breaking the C–O bonds of ethoxide species as follows:

$$O_{(l)} + CH_3CH_2O\text{–}U^{x+} + V_o \rightarrow OH_{(s)} + CH_2CH_2 + O_{(s)}$$

where (s) and (l) denote surface and lattice species, respectively, while V_o represents a surface oxygen vacancy.

The production of butene can be explained by the reductive coupling of two acetaldehyde molecules. Butene was observed from acetaldehyde over Ar^+-sputtered $TiO_2(0\,0\,1)$ [21], as well as from the reaction of acetic acid over an e^--sputtered surface of a $UO_2(1\,1\,1)$ single crystal [4]. It is also worth noting that organometallic complexes of U are active for the reductive coupling reaction [22]. The formation of ketene coincided with the development of traces of acetate species in the C 1s spectrum, indicative of some oxidation of ethoxide species (the oxygen required to oxidise ethoxide species is most likely provided from the reductive coupling route). The formation of ketene from acetic acid has been previously observed over several oxides including $TiO_2(0\,0\,1)$ [23], $CeO_2(1\,1\,1)$ [24], and $UO_2(1\,1\,1)$ [4]. The formation of acetone was not anticipated, but has been reported by Kim and Barteau [23] under UHV conditions for the reaction of acetic acid on the $\{1\,1\,4\}$-faceted $TiO_2(0\,0\,1)$ surface. The proposed reason for the ketonisation of acetic acid was the presence of doubly coordinately unsaturated cations, and the tendency of the surface to deoxygenate the surface carboxylate species. By analogy, upon sputtering with Ar^+, a small fraction of U^{x+} ($x = 4$ or lower) may contain double coordination vacancies, accommodating two acetates and initiating the ketonisation reaction.

Overall, the chemistry of ethanol on this Ar^+-sputtered surface is essentially governed by the presence or absence of oxygen anions.

5. Conclusions

The reactions of ethanol have been studied on the Ar^+-sputtered surface of a $UO_2(1\,1\,1)$ single crystal using TPD, supplemented by XPS, under UHV conditions. Two dehydrogenation (to acetaldehyde) and dehydration (to ethylene) channels were observed, one at 575 K with a ratio of 0.96 (similar to that previously observed over stoichiometric $UO_2(1\,1\,1)$ [6]), while the other was attributed to U suboxide sites, and yielded twice as much ethylene as acetaldehyde. The driving force for the latter reaction channel appears to be the restoration of oxygen anion sites. In addition to the dehydrogenation and dehydration pathways, several minor reactions were observed. These were: (1) oxidation to acetates followed by dehydration (ketene) and ketonisation (acetone), and (2) reduction to acetaldehyde followed by coupling to butene.

Acknowledgements

The authors, especially SVC, would like to thank Adrian Sherrill (University of Delaware) for his assistance in all the data acquisition on the VG Scientific surface analysis system, and also the financial support from The University of Auckland and The New Zealand Institute of Chemistry.

References

[1] K.S. Schulz, D.F. Cox, J. Phys. Chem. 97 (1993) 647.
[2] L. Gamble, L.S. Charles, C.T. Campbell, Surf. Sci. 348 (1996) 1.
[3] J. Jacobs, W. Mokwa, D. Kohl, G. Heiland, Vacuum 33 (1983) 869.
[4] S.V. Chong, H. Idriss, J. Vac. Sci. Technol. A 18 (2000) 1900.
[5] A.S. Eppler, G. Rupprechter, A. Avoyan, G.A. Somorjai, in: Proceedings of the 16th NAM Catalysis Society, Boston, 30 May–4 June, 1999, Technical Program, p. 40.
[6] S.V. Chong, T.R. Griffiths, H. Idriss, Surf. Sci. 444 (1999) 187.
[7] W.P. Ellis, T.N. Taylor, Surf. Sci. 75 (1978) 279.
[8] K.A. Thompson, W.P. Ellis, T.N. Taylor, S.M. Valone, C.J. Maggiore, Nucl. Instrum. Meth. Phys. Res. 218 (1983) 475.

[9] C. Muggelburg, M.R. Castell, G.A.D. Briggs, D.T. Goddard, Surf. Rev. Lett. 5 (1998) 315.

[10] G.C. Allen, P.A. Tempest, J.W. Tyler, J. Chem. Soc., Faraday Trans. 1 (83) (1987) 925.

[11] H. Madhavaram, P. Buchanan, H. Idriss, J. Vac. Sci. Technol. A 15 (1997) 1685.

[12] G.C. Allen, P.M. Tucker, J. Chem. Soc., Dalton Trans. (1973) 470.

[13] J.R. Naegele, J. Ghijen, L. Manes, Struct. Bonding 59/60 (1985) 197.

[14] T. Gouder, C.A. Colmenares, J.R. Naegele, Surf. Sci. 342 (1995) 299.

[15] J.A. Lloyd, W.L. Manner, M.T. Paffett, Surf. Sci. 423 (1999) 265.

[16] K.S. Kim, M.A. Barteau, J. Mol. Catal. 63 (1990) 103.

[17] J.M. Vohs, M.A. Barteau, Surf. Sci. 221 (1989) 590.

[18] K.S. Kim, M.A. Barteau, J. Catal. 125 (1990) 353.

[19] X.D. Peng, M.A. Barteau, Catal. Lett. 7 (1990) 395.

[20] X.D. Peng, M.A. Barteau, Surf. Sci. 224 (1989) 327.

[21] H. Idriss, K.S. Kim, M.A. Barteau, J. Catal. 139 (1993) 119.

[22] G.M. Smith, H. Suzuki, D.C. Sonnenberger, V.W. Day, T.J. Marks, Organometallics 5 (1986) 549.

[23] K.S. Kim, M.A. Barteau, J. Catal. 125 (1990) 353.

[24] J. Stubenrauch, E. Brosha, J.M. Vohs, Catal. Today 28 (1996) 433.